SIGNAL DETECTION IN FIXED PATTERN CHROMATIC NOISE

A. J. Ahumada, Jr. and W. K. Krebs
NASA Ames Research Center, Moffett Field, CA and Naval Postgraduate School, Monterey, CA.
AAhumada@mail.arc.nasa.gov, WKrebs@nps.navy.mil

Introduction

This study is part of a project to develop image discrimination models that can predict the detectability of target signals in color images. Image discrimination models take as input two images and predict the number of just-noticeable differences (JNDs) between the images. If one image is a background image and the other image has the identical background plus a target image, the model predicts the detectability of the target signal in the background.

Previous work with luminance targets in complex imagery has shown that target detectability is strongly influenced by variations in background contrast. The goal of this study is to measure the masking of targets by fixed-pattern chromatic noise. These measurements simplify the testing and calibration of the contrast masking components of color image discrimination models.

Methods

Observers. The 10 observers were students at the Naval Postgraduate School and received course credit for their participation. They had passed standard tests for acuity and color vision.

Stimuli. The stimuli were presented using the red and green guns of a color CRT, whose responses were linearized by lookup tables feeding 10 bit DACs. At full output, the red gun gave a luminance Y = 18.5 cd/m^2, and CIE color coordinates (x, y) = (0.616, 0.337). The corresponding green gun values were Y = 70.7 cd/m^2 and (x, y) = (0.293, 0.604). The screen background was set to a yellow with equal luminance contributions from the red and green guns, with Y = 18.4 cd/m^2 and (x, y) = (0.346, 0.252). These calibrations were done with a Minolta CS-100. The screen was viewed from a distance of 1 m, giving 52.7 pixels per degree of visual angle in the horizontal direction and 37.6 pixels per degree vertically. The screen was 19.4 by 13.6 deg (1024 by 512 pixels).

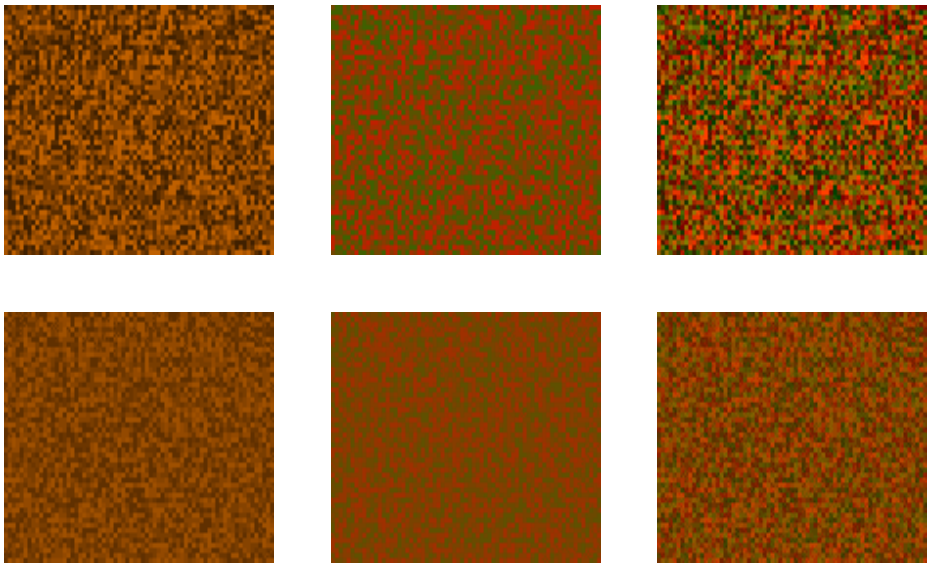

Figure 1. (Top row) The high contrast maskers. (Left to right) Luminance mask, red/green mask, sum of the two masks. (Bottom row) The corresponding low contrast maskers.

The fixed pattern noise images were 2.62 by 2.66 deg (138 by 100 pixels). They were generated as 69 by 50 pixel images and then pixel replicated. The luminance mask pixels had the same chromaticity coordinates as the background. The contrast values were selected randomly from 6 luminance values equally spaced around the background luminance. The red pixels of red/green masks were generated the same way, but the green pixel contrasts were reversed to keep the physical luminance constant. The noise sample forming the red/green mask was different from that of the luminance mask. A mask varying in luminance and chromaticity was generated by summing the luminance and the red/green masks in the contrast domain. A separate lower contrast set of three masks was similarly formed using two new random pixel sequences at half the contrast. For the high contrast set, the peak contrast was 0.5.

Figure 2. (Left) Luminance target on the uniform background. (Right) Red/green target on the uniform background.

Two target signals were used, a luminance and a red/green target. They were uniform squares 0.266 by 0.266 deg (14 by 10 pixels). The luminance target was the background yellow. The luminance target was the background yellow. For the red/green target, the green gun level decreased as the red increased, keeping the luminance constant. The color of the red/green target varied from red to the background yellow as the target contrast (defined as the red signal contrast) was lowered. The targets were mixed with the masks by interleaving frames at 120 frames per second, so the actual peak contrasts of the high contrast noises were 0.25.

Procedure. Thresholds were measured on the uniform yellow background and on the six fixed pattern noise backgrounds (2 contrast levels by 3 patterns: luminance noise (Y), isoluminant red-green noise (R), and the sum of the luminance and red/green masks (S). Thresholds were estimated using a two-interval forced-choice (2IFC) QUEST procedure for blocks of 30 trials. The signal and no-signal intervals were each 0.5 sec in duration and separated by an interval of 0.1 sec. The next trial began 0.25 sec after the response to the previous trial. A feedback tone indicated an incorrect response. Horizontal and vertical lines outside the masking image region indicated the position of the possible target during the trial. Each observer ran one practice day and three test days. On each day the observer completed a warm-up session of 5 blocks of conditions chosen at random without replacement from the 14 conditions (2 signals by 7 maskers), and then ran one block for each masking condition in a random order. Following the warm-up session the observer completed one 30 trial block for each masking condition in a random order. The median threshold contrast was found from the three measurements in each condition and for each observer the masking effect of each masker was represented in decibels as 20 times the logarithm to the base ten of the ratio of the masked threshold to the unmasked threshold.

Results

Confidence intervals (95%) for the average thresholds on the uniform background in dB re 10^{-6} deg^2 sec of contrast energy) were 8.8± 2.0 dBB for the luminance target and 12.2± 3.5 dBB for the red/green target. Figure 3 shows for both targets the ratios in dB of the mean masked thresholds to that of the uniform background. Error bars are 95% confidence limits based on the variance of the masking scores over observers averaged over maskers. Both targets show clear masking by the corresponding masks; the

luminance mask masked the luminance target and the red/green mask masked the red/green target (bars marked YY and RR in the figure). The masking of the luminance target by the red/green noise (YR) was small, but statistically significant (4.1 ± 3.0 dB). However, the luminance noise alone did not mask the red/green target (RY), and the increased masking by the sum mask (RS) over that of the red/green mask alone (RR) is not significant (4.1 ± 5.0 dB), so there is no strong evidence for luminance masking of the red/green target. The average difference for the high and low contrast maskers was 4.0 ± 1.4 dB.

Figure 3. Threshold increases in dB for the 6 maskers on the two signals. The error bars, 95% confidence intervals for these increases, are plus and minus 3.0 dB.

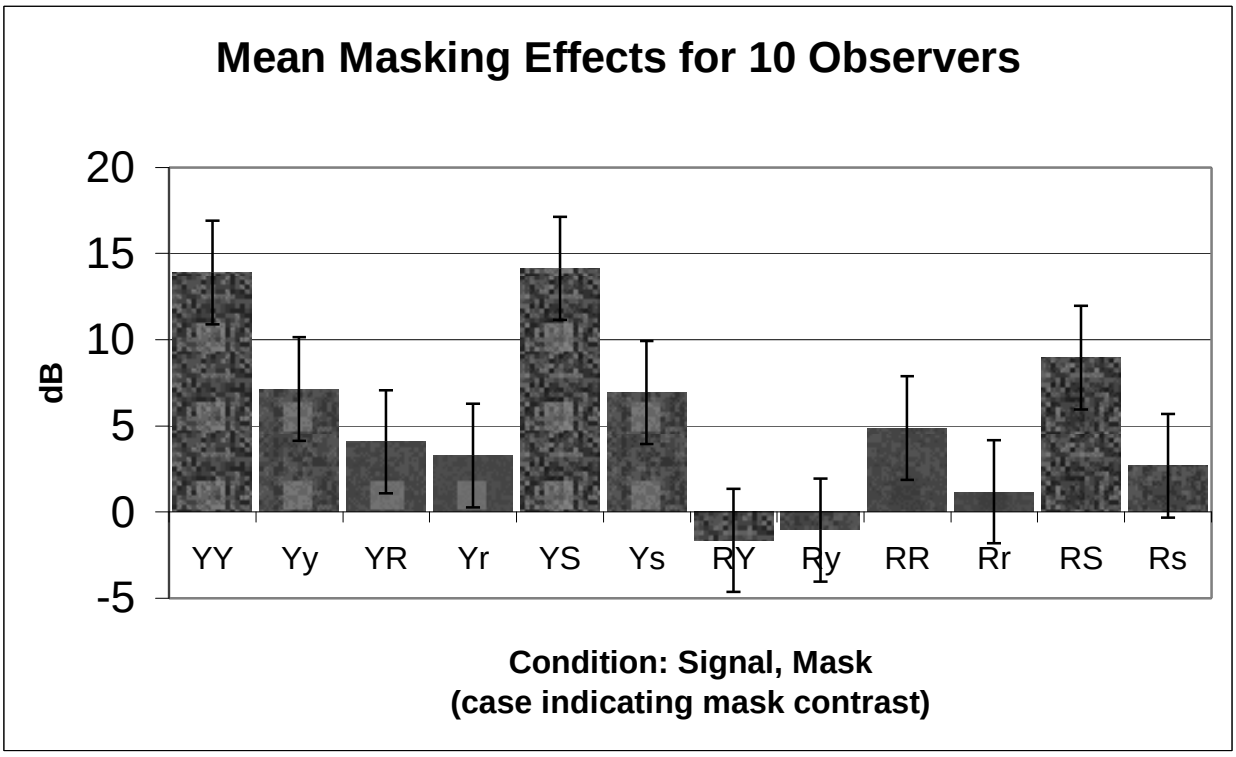

Predictions of an Independent Channels Model

Figure 4 shows predictions for the data of Figure 1 by an image discrimination model with contrast masking separately in the luminance and red-green channels. They can be compared with the observer results. The masking level parameters could have been chosen to fit the data better. Only the prediction of no masking of the luminance target by the red/green noise (YR) is outside the observer data confidence interval. The average noise contrast level effect is predicted to be 3.1 dB, also in its confidence interval.

The model. The model begins by the conversion of RGB images to CIE XYZ images. The Y image is the luminance channel image and the Z image is used as a blue channel image and a red-green opponent channel image O is computed as O = 0.47 X - 0.37 Y - 0.10 Z. Next the images are converted to contrast images. The luminance contrast image Y_C is computed by $Y_C = (Y-y_0)/ y_0$, where y_0 is the average luminance of the no-target image. The opponent contrast image is computed as $O_C = (O-o_0)./Y$, where o_0 is the average of the no-target opponent image and ./ indicates pixel by pixel division. Similarly $Z_C = (Z-z_0)./Y$. These images are contrast sensitivity filtered. Unmasked threshold predictions are computed from the Minkowski distance between the filtered target and no-target images in each channel. Masking

coefficients are computed from the RMS value of the filtered no-target images in each channel. For the channel with masking within each channel, these coefficients are simply (1+ (RMS(Y_C)/Y_M)^2)^-0.5, (1+ (RMS(O_C)/O_M)^2)^-0.5, and (1+ (RMS(Z_C)/Z_M)^2)^-0.5. The values Y_M, O_M, and Z_M are the contrast masking contrast thresholds for each channel. When the RMS contrast is equal to the masking threshold, the masking factor lowers the threshold 3 dB. The masking threshold values can be estimated from the observed masking factors shown in Figure 3.

Luminance signal predictions. The model predicts no masking of the luminance signal by the isoluminant noise. The luminance channel predictions are easy to understand because the chromatic masks play no role in the prediction. The luminance target generates no unmasked target difference in the chromatic channels on the uniform background or luminance masks and negligible difference when chromatic noise is present.

Isoluminant signal predictions. The luminance masks play a small "unmasking" role for the red/green target because the strength of the opponent signal is inversely proportional to the local luminance, contributing more to the signal when the luminance is low than it loses when the luminance is high.

Simpler models with linear chromatic channels were tested. They predicted masking of the luminance mask alone on the red/green target because it generates masking variation in the opponent channel.

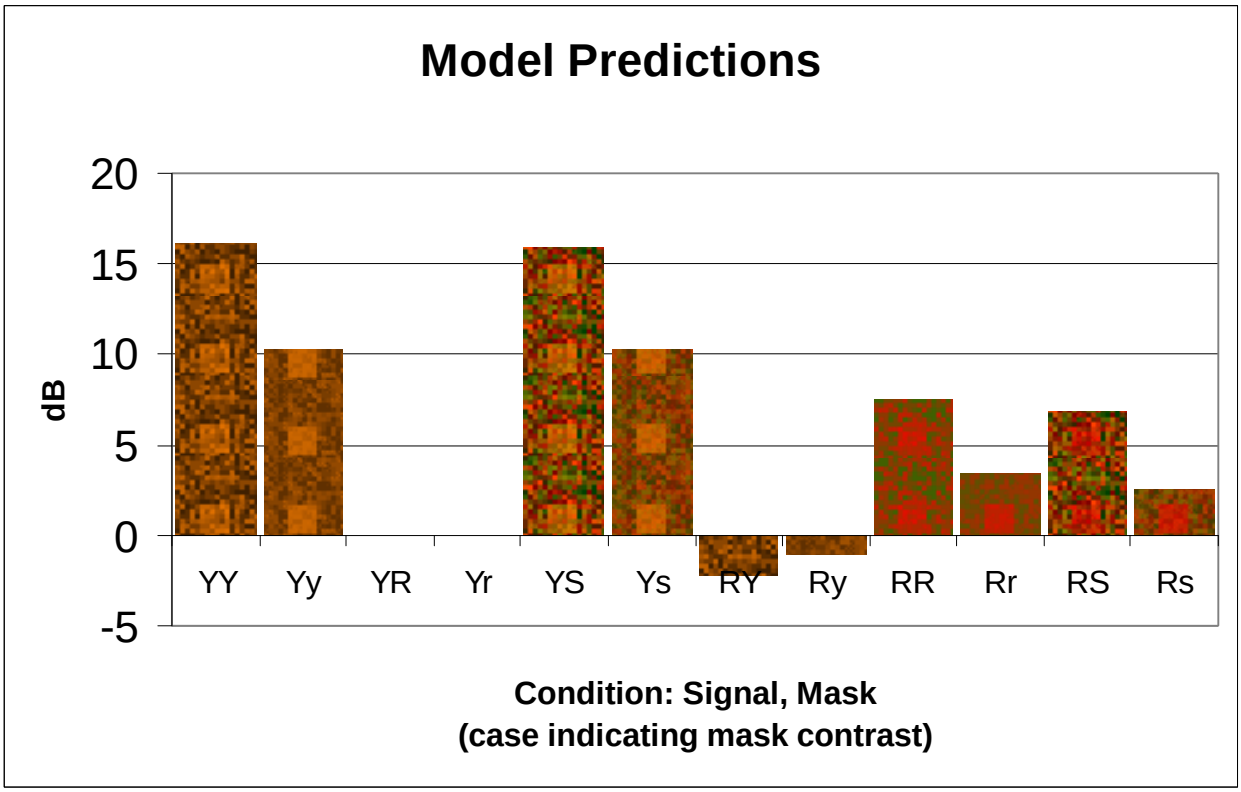

Conclusions

The main masking was by the mask in the same color direction as the target. Luminance masks did not raise the red/green target threshold. Red/green masking of the luminance target was small, but significant. The results with the sum masks suggests that this masking of luminance signals by red/green masks could only be seen with masking imagery of very low luminance contrast. Thus, in applications with substantial

luminance in the masking imagery, masking should be was fairly well predicted by models with contrast masking within channels only.

Chromaticity channel models that normalize by the local luminance fit these results better than do models with linear or globally normalized chromatic channels. Local models can predict a small facilitation of chromatic signal detection by local luminance variation.

References

Albert J. Ahumada, Jr., Bettina L. Beard (1998) A simple vision model for inhomogeneous image quality assessment, in Society for Information Display Digest of Technical Papers, ed. J. Morreale, vol. 29, Paper 40.1, Santa Ana, CA.

Albert J. Ahumada, Jr., Bettina L. Beard (1997) Image discrimination models predict detection in fixed but not random noise, Journal of the Optical Society of America, 14, pp. 2471-2476.

Albert J. Ahumada, Jr. (1996) Simplified vision models for image quality assessment, in Society for Information Display International Symposium Digest of Technical Papers, ed J. Morreale, Volume 27, pp. 397-400, Society for Information Display, Santa Ana, CA.

Kjell Brunnström, Robert Eriksson, Albert J. Ahumada, Jr. (1999) Spatio-temporal discrimination model predicting IR target detection, in Human Vision and Electronic Imaging III, ed. B.E. Rogowitz and T.N. Pappas, Proceedings Volume 3644, pp. 403-410, SPIE, San Jose, CA.

Miguel P. Eckstein, Andrew. B. Watson, Albert J. Ahumada, Jr. (1997) Visual signal detection in structured backgrounds. II. Effects of contrast gain control, background variations, and white noise, Journal of the Optical Society of America, 14, (9), pp. 2406-2419.

Miguel P. Eckstein, Albert J. Ahumada, Jr., Andrew. B. Watson (1997) Image discrimination models predict signal detection in natural medical image backgrounds, in Human Vision, Visual Processing, and Digital Display VIII, ed. B.E. Rogowitz and T.N. Pappas, Proceedings Volume 3016, pp. 44-56, SPIE, Bellingham, WA.

Heidi A. Peterson, Albert J. Ahumada, Jr., Andrew B. Watson (1993) An improved detection model for DCT coefficient quantization, in Human Vision, Visual Processing, and Digital Display IV, ed. B.E. Rogowitz and J. Allebach, Proceedings Volume 1913, pp. 191-201, SPIE, Bellingham, WA.

Ann Marie Rohaly, Albert J. Ahumada, Jr., Andrew B. Watson (1997) Object Detection in natural backgrounds predicted by discrimination performance and models, Vision Research, 37, pp. 3225-3235.

Lauren F. V. Scharff, Albert J. Ahumada, Jr., Alyson L. Hill (1999) Discriminability measures for predicting readability, in Human Vision and Electronic Imaging III, ed. B.E. Rogowitz and T.N. Pappas, Proceedings Volume 3644, pp. 270-277, SPIE, San Jose, CA.

Andrew B. Watson, J.Q. Hu, J.F. McGovan III, J.B. Mulligan (1999) Design and performance of a digital video quality metric, in Human Vision and Electronic Imaging IV, ed. B.E. Rogowtiz and T.N. Pappas, Proceedings Volume 3644, pp. paper 17, SPIE.